

https://doi.org/10.1070/QEL16625

Modelling the spectral characteristics of 1.5–1.6 μm high-power asymmetric-waveguide single-mode laser diodes

V.D. Kurnosov, K.V. Kurnosov

Abstract. **Spectral characteristics of high-power single-mode laser diodes with a radiation wavelength of 1.5–1.6 μm are simulated with allowance for nonlinear losses. A satisfactory agreement between the calculation and experimental results as applied to the dependence of the wavelength and radiation spectrum width on the laser pump current is demonstrated. The effect of thermal resistance of a laser diode on the active region heating, spectrum width, and radiation wavelength is considered.**

Keywords: *single-mode laser diodes, radiation spectrum width.*

1. Introduction

It is known that high-power laser diodes (LDs) have a wide emision spectrum [1–4]; a review of their characteristics is presented in [5]. Pikhtin et al. [6] explain the phenomenon of inhomogeneous broadening of the emission spectra of LDs based on quaternary solutions by their spinodal decay. However, this hypothesis has not been confirmed experimentally. It is noted in [7] that there are no known works dedicated to the study of the causes leading to an increase in the emission spectrum width in LDs at high pump levels. There are several features in the spectrum development, which manifest themselves with increasing pump current: the spectrum shifts to the long-wavelength region, which is due to the heating of the active region, the short-wavelength spectral boundary shifting as well. In some cases, at a pump current density of 80–100 kA cm^{-2}; the emission spectrum width reaches 60 nm.

Another important feature is the saturation of the intensity maximum of the emission spectrum. Upon reaching a certain value of the pump current density, the laser intensity ceases to increase, and the emission spectrum broadening is only observed. There are no obvious reasons that could explain this effect. The works dedicated to the multimode lasing regime cannot explain the occurrence of at least 750 longitudinal modes (the intermode distance is 0.8 Å) in the LD with a resonator length of 1.5 mm. The emission spectrum broadening up to 50–60 nm is possible only if threshold conditions for the higher energy levels are fulfilled relative to those already involved in the lasing. For this, the concentration of current carriers at the higher levels should be increased to the threshold value.

Vorob'ev et al. [8] present calculated spectra of spontaneous emission at a temperature $T = 77$ K [8]; however, there is no calculation of stimulated emission spectra (only experimental lasing spectra are presented). The features of emission spectra and thermal resistance of cw LDs are considered in [9].

In the present work, the wavelength and width of LD emission spectrum are simulated with allowance for nonlinear losses (or spectral burning of carriers) in rate equations. Experimental data on the spectral and power characteristics of LDs are taken from [10].

2. Calculation of LD spectral characteristics

When performing the calculations, we use stationary solutions of the system of rate equations, similar to that considered in [11]:

$$\frac{\mathrm{d}S_m}{\mathrm{d}t} = \left[G_m(1-\varepsilon S_m) - \frac{1}{\tau_{\mathrm{ph}}}\right]S_m + \beta R_{\mathrm{sp}} - \gamma S_m^2, \tag{1}$$

$$\frac{\mathrm{d}n_{\mathrm{a}}}{\mathrm{d}t} = \frac{I}{eV_{\mathrm{a}}} - R_{\Sigma} - \sum G_m(1-\varepsilon S_m)S_m, \tag{2}$$

where S_m, G_m are the photon density and the gain of the mth mode in the LD resonator; τ_{ph} is the lifetime of photons in the resonator; n_{a} is the carrier density in the active region; β is the coefficient that takes into account the contribution of spontaneous emission to the lasing mode; γ is the nonlinear loss; ε is the coefficient that takes into account the spectral burning of carriers; R_{sp} is the rate of spontaneous recombination; R_{Σ} is the total rate of radiative and nonradiative recombination; V_{a} is the volume of the active laser region; and I is the pump current.

We should note that system (1), (2) differs from the system of rate equations from Ref. [11], in which the equation for the carrier density does not contain the optical confinement factor.

The calculations below are based on the results of work [12], where it is shown that the best agreement between theory and experiment is obtained for models without inversion of masses and with radiative transitions without fulfilling the selection rule. In the transition model without the selection rule for the wave vector, the gain is defined as

$$g(h\nu) = G_0 \sum_i \sum_{n,k} \left[m_{\mathrm{h}i} \ln \left(\frac{1+\exp\left(\dfrac{F_{\mathrm{c}} - h\nu - E_{\mathrm{v}ni}}{k_{\mathrm{B}}T}\right)}{1+\exp\left(\dfrac{F_{\mathrm{c}} - E_{\mathrm{c}ni}}{k_{\mathrm{B}}T}\right)} \times \right.\right.$$

V.D. Kurnosov, K.V. Kurnosov Open Joint-Stock Company M.F. Stel'makh Polyus Research Institute, ul. Vvedenskogo 3, stroenie 1, 117342 Moscow, Russia; e-mail: webeks@mail.ru

Received 5 February 2018; revision received 28 April 2018
Kvantovaya Elektronika **48** (9) 807–812 (2018)
Translated by M.A. Monastyrskiy

$$\times\frac{1+\exp\left(\dfrac{F_v+h\nu-E_{cki}}{k_BT}\right)}{1+\exp\left(\dfrac{F_v-E_{vki}}{k_BT}\right)}\Bigg]\Bigg], \quad (3)$$

where G_0 is the coefficient determined by formula (23) in work [12]; $E_{cni} = E_{c0} + E_{cn}$; $E_{vni} = E_{v0} - E_{vin}$; the subscript i = h, l refers to heavy and light holes; and the summation subscript n, k are the numbers of subzones in the quantum well.

In performing the calculations, it was assumed that the energies of Fermi quasi-levels within the conduction band (F_c) and the valence band (F_v) are related by the electro-neutrality equation determined by formula (11), while the electron and hole densities in the laser active region (n_a, p_a) and in the waveguide layer (n_w, p_w) are determined by formulas (12), (13) from work [12]. The calculations took into account the narrowing of the $Ga_yAl_xIn_{1-x-y}As$ band gap in the active region E_{ga} and in the waveguide layers E_{gw} under pumping the laser structure by the current. The calculation was carried out using formula (14) from work [12].

The dependence of the band gap E_g in the $Ga_yAl_xIn_{1-x-y}As$ layers was calculated using formula (3) from [13]:

$$E_g(Ga_yAl_xIn_{1-x-y}As) = xE_g(AlAs) + yE_g(GaAs)$$
$$+ (1-x-y)E_g(InAs) - xyK_{AlGaAs} - y(1-x-y)K_{GaInAs}$$
$$- x(1-x-y)K_{AlInAs}, \quad (4)$$

where $K_{AlGaAs} = 0.399$, $K_{GaInAs} = 0.44$, and $K_{AlInAs} = 0.614$ are the parameters of nonlinearity of the corresponding triple solid solutions.

The dependence of E_g on the temperature of two-component solutions is taken in the form [14]

$$E_g(InAs) = 0.417 - \frac{2.76\times10^{-4}T^2}{T+93},$$
$$E_g(AlAs) = 3.099 - \frac{8.85\times10^{-4}T^2}{T+530}, \quad (5)$$
$$E_g(GaAs) = 1.519 - \frac{5.405\times10^{-4}T^2}{T+204}.$$

The lifetime of photons in the resonator is

$$\tau_{ph} = (v_{gr}\alpha)^{-1}, \quad (6)$$

where v_{gr} is the group velocity of light.

Losses in the laser are

$$\alpha = \alpha_{out} + \Gamma_a\alpha_a + \Gamma_w\alpha_w + (1-\Gamma_a-\Gamma_w)\alpha_{em}, \quad (7)$$

where $\alpha_{out} = L^{-1}\ln[(R_1R_2)^{-1/2}]$; L is the laser resonator length; R_1 and R_2 are the mirror reflection coefficients; and Γ_a and Γ_w are the optical confinement factors of the active region and waveguide layers. Losses on free carriers in the active region (α_a), waveguide (α_w) and emitter (α_{em}) layers were determined by formula (19) from Ref. [12].

It is should be noted that the optical confinement factors of the waveguiding p and n layers differ from each other in the case of an asymmetric waveguide. The calculation shows that the optical field maximum is shifted to the middle of the n waveguide, and the optical confinement factor of the waveguiding p layer is less than that of the waveguiding n layer. The calculations make use of the total optical confinement factor of the waveguiding p and n layers. The optical power from one face of the resonator is given by the expression

$$P = \sum P_m = \frac{1}{2}h\nu\frac{V_a}{L}v_{gr}\ln\frac{1}{R_1R_2}\sum S_m, \quad (8)$$

where P_m is the optical radiation power of the mth mode.

In accordance with work [15], we represent the spontaneous recombination rate in the quantum well in the form

$$R_{spa} = B_{spa}\left(\frac{T_0}{T_0+\Delta T_{LD}}\right)\frac{n_ap_a}{1+(n_a+p_a-\sqrt{n_ap_a})/N_a^*}, \quad (9)$$

and the spontaneous recombination rate in the waveguide in the form

$$R_{spw} = B_{spw}\left(\frac{T_0}{T_0+\Delta T_{LD}}\right)^{3/2}\frac{n_wp_w}{1+(n_w+p_w-\sqrt{n_wp_w})/N_w^*}, \quad (10)$$

where $N_i^* = 0.25[(m_{ei}=m_{hhi})k_BT/(\pi\hbar^2)]^{3/2}$; B_{spi} are constant coefficients; i = a, w; ΔT_{LD} is the heating of the active region; and T_0 is the radiator temperature.

The laser pump current is determined by the formula

$$I = qV_a\left[R_a + v_{gr}\sum_m G_mS_m\right] + qV_wR_w + qV_aDn_a^{5.5}. \quad (11)$$

The last term in (11) takes into account the leakage current [16]; q is the electron charge. The rates of radiative and nonradiative recombination in the active region and in the waveguiding layers R_a and R_w are expressed as

$$R_i = An_i + R_{spi} + C_0\exp\left[\frac{\Delta E}{k_B}\left(\frac{1}{T_0}-\frac{1}{T}\right)\right]$$
$$\times(n_i^2p_i + n_ip_i^2), \quad i = a, w, \quad (12)$$

where A, C_0, and ΔE are constant coefficients.

For the stationary case of the rate equation (1) and $\varepsilon = 0$, the volume density of photons S_m with the energy E_m in the mth mode is expressed as

$$v_{gr}(G_m-\alpha)S_m + \beta R_{sp} - \gamma S_m^2 = 0, \quad (13)$$

where $G_m = \Gamma_a g(E_m)$.

The temperature of the LD active region can be written as

$$T = T_0 + \Delta T_{LD}(I, P, \Delta T). \quad (14)$$

Here $\Delta T_{LD}(I, P, \Delta T)$ is the heating of the LD active region due to flowing pump current and the radiation power coupled out from the resonator; and ΔT is the change in the radiator temperature (the temperature T_0 was kept constant).

We assume that the thermal resistance R_T depends on the temperature as follows [16]:

$$R_T(\Delta T_{LD}) = R_{T0}\left(\frac{T_0+\Delta T_{LD}}{T_0}\right)^{\varkappa}, \quad (15)$$

where $\varkappa$ is a constant value; and R_{T0} is thermal resistance at a radiator temperature $T = T_0$.

The heating of the LD active region is written in the form

$$\Delta T_{\rm LD}(I,P,\Delta T) = R_{\rm T}(\Delta T_{\rm LD})[U(I,\Delta T_{\rm LD})I - P] + \Delta T, \quad (16)$$

where U is the LD voltage drop.

The value of the thermal resistance of the 'LD active region–radiator' transition used in the calculation is defined as $R_{\rm T0} = R_{\rm LD} + R_{\rm rad}$, where $R_{\rm rad}$ is the radiator's thermal resistance (together with the LD housing). The value $R_{\rm rad}$ = 4.8 K W^{-1} for the LD mounted in the housing with a diameter of 11 mm is borrowed from Ref. [16].

Thermal resistance between the LD active region and the contact plate is calculated by the formula [17]

$$R_{\rm LD} = \frac{1}{k_{\rm T0}\pi L}\ln\frac{16h_{\rm LD}}{\pi w}, \quad (17)$$

where $k_{\rm T0}$ is the coefficient of thermal conductivity at the temperature $T = T_0$; $h_{\rm LD}$ is the LD crystal height; and w is the strip contact width. It is assumed in the calculations that at w = 3 μm, $h_{\rm LD}$ = 100 μm, and L = 1.6 mm, the thermal resistance is $R_{\rm T0}$ = 21 K W^{-1} with allowance for the thermal conductivity of the InP and $Al_xGa_yIn_{1-x-y}As$ layers [14].

The LD voltage is a nonlinear function of the pump current and LD heating:

$$U(I,\Delta T_{\rm LD}) = U_{\rm cut}(\Delta T_{\rm LD}) + IR_{\rm g}(I), \quad (18)$$

$$U_{\rm cut}(\Delta T_{\rm LD}) = U_{\rm 0cut}(1 - T_{\rm u}^{*}\Delta T_{\rm LD}), \quad (19)$$

$$R_{\rm g}(I) = R_{\rm g0}(1 - R_{\rm g}^{*}I), \quad (20)$$

where $U_{\rm 0cut}$ is the cutoff voltage determined by the linear approximation of the experimental light–current characteristic for the pump current tending to zero; $R_{\rm g}$ is the LD dynamic resistance; and $T_{\rm u}^{*}$ and $R_{\rm g}^{*}$ are constant coefficients. We assume that the cutoff voltage depends only on temperature, while the LD dynamic resistance depends only on the pump current. The experimental and calculated characteristics are compared for the LD with a resonator length of 1.6 mm, investigated in [10].

The calculation was performed for the 351st mode (175 modes on the right and on the left of the laser mode generated with a maximal amplitude). Figure 1 shows experimental emission spectra of the LD with L = 1.6 mm at pump currents (laser powers) of 1213 mA (300 mW), 253 mA (60 mW), and 95 mA (5 mW) measured at the LD radiator temperature T_0 = 20 °C (taken from work [10]). Figure 2 displays the calculated spectra at the pump currents indicated in Fig. 1 and $\varepsilon = 0$, $\gamma = 0$, and Fig. 3 demonstrates the calculated spectra at the same pump currents and $\varepsilon = 0$, $\gamma = 6\times10^{-8}$ cm^3 s^{-1}. Note that in Figs 1–3, the same wavelength range of 16 nm is plotted along the horizontal axis.

The emission wavelength and the spectrum width were calculated for the half-amplitude of the maximum generating mode at different values of the coefficient γ that determines the nonlinear losses. Figure 4 shows the calculated dependences of the laser wavelength, active region heating, and thermal resistance on the pump current for $\varkappa$ = 1.4, 0, –2.5, –10 [see Eqn (15)] and T_0 = 20 °C. For comparison, Fig. 4a presents the experimental points of the dependence of laser wavelength on the pump current, borrowed from [10].

Figures 5 and 6 show, respectively, the experimental and calculated dependences of the laser wavelength and the

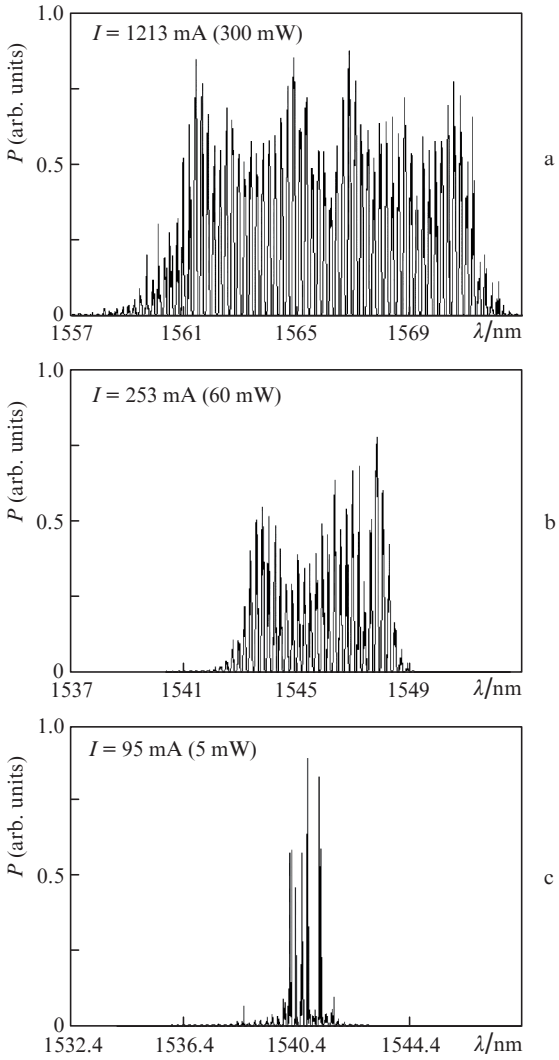

Figure 1. Experimentally measured LD emission spectra with a resonator length of 1.6 mm at pump currents (laser powers) of (a) 1213 mA (300 mW), (b) 253 mA (60 mW), and (c) 95 mA (5 mW).

dependences of the emission spectrum width at half-height on the pump current for T_0 = 20, 30, and 40 °C, L = 1.6 mm, and $\varkappa = -2.5$.

The calculated dependences of the wavelength and emission spectrum width on the coefficient γ that determines the nonlinear losses for a pump current of 1213 mA (300 mW) are given in Fig. 7.

Figure 8 displays the experimental and calculated voltage-current and light–current characteristics in the LD at $\gamma = 6\times10^{-7}$ cm^3 s^{-1}, $\varepsilon = 0$.

3. Discussion of the results

In Eqn (7) of this paper, we have neglected the losses on free carriers in the waveguide considered in [18]:

$$\alpha(I) = (\sigma_{\rm e} + \sigma_{\rm h})\left[\frac{I}{2qwL}\left(\frac{L_{\rm n}}{D_{\rm e}} + \frac{L_{\rm p}}{D_{\rm h}}\right)\right], \quad (21)$$

where I is the pump current; $\sigma_{\rm e(h)}$ are the absorption cross sections for electrons (holes); $L_{\rm n}$ and $L_{\rm p}$ are defined by formulas (8) and (9) in work [18]; and $D_{\rm e}$ = 200 cm^2 s^{-1} and $D_{\rm e}$ =

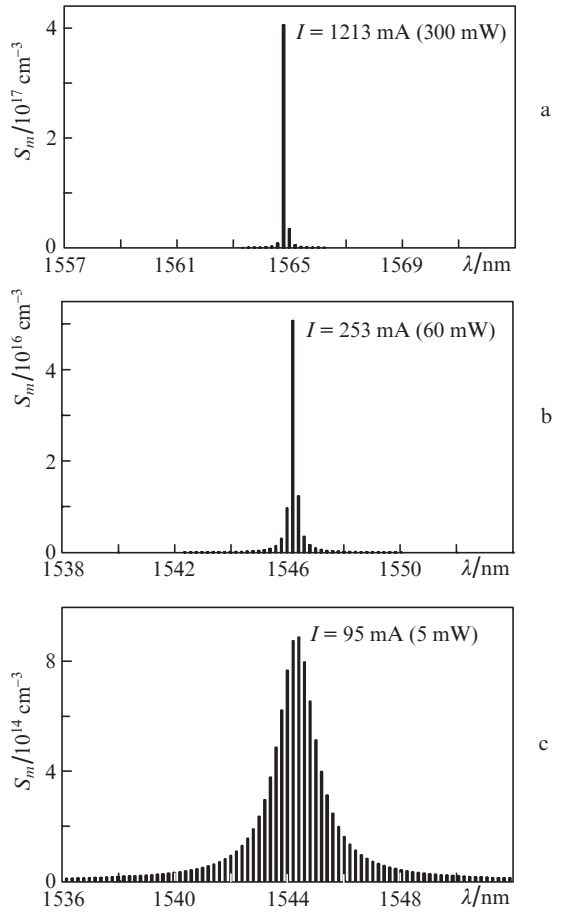

Figure 2. Calculated spectra at the same pump currents (laser powers) as in Fig. 1, and $\varepsilon = 0$, $\gamma = 0$ (S_m is the volume density of photons).

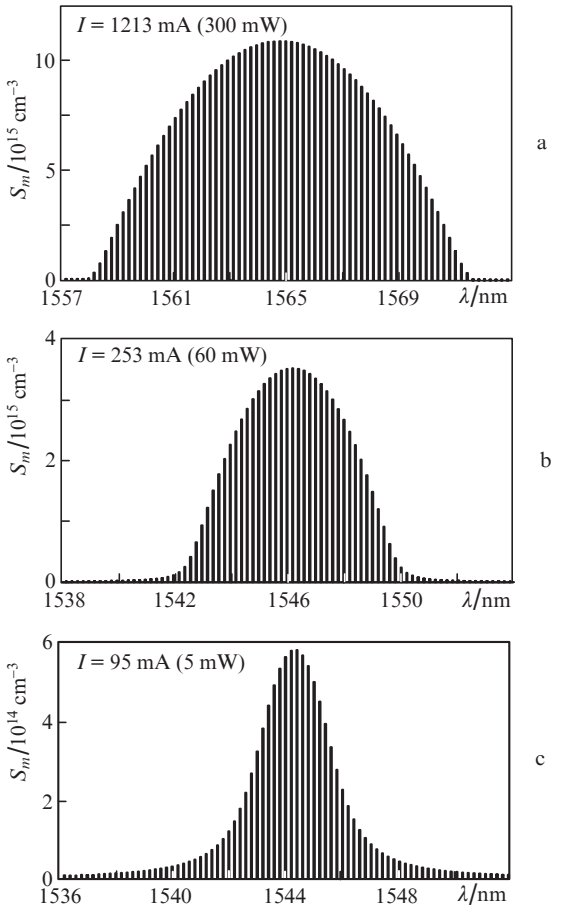

Figure 3. Calculated spectra at the same pump currents (laser powers) as in Fig. 1, and $\varepsilon = 0$, $\gamma = 6 \times 10^{-8}$ cm^3 s^{-1}.

10 cm^2 s^{-1} are the diffusion coefficients of electrons and holes, respectively. For the maximum pump current $I = 1.3$ A, the losses are $\alpha(1.3) = 1$ cm^{-1}, which is more than an order of magnitude less than the losses determined by formula (7).

It can be seen from Fig. 2c that the calculated emission spectrum in the case $\varepsilon = 0$ and $\gamma = 0$ has several longitudinal modes at a pump current of 95 mA (5 mW) and a virtually single-frequency lasing mode at a current of 1213 mA (300 mW). Thus, as the pump current increases, the emission spectrum narrows rather than broadens, which does not agree with the experiment. On the contrary, at $\varepsilon = 0$, $\gamma = 6 \times 10^{-8}$ cm^3 s^{-1} we observe the broadening of the emission spectrum when the LD pump current (power) increases. Comparing the experimental dependences shown in Fig. 1 with the calculated dependences in Fig. 3, we can see a satisfactory agreement between theory and experiment.

Taking into account the spectral burning of carriers ($\gamma = 0$ and $\varepsilon = 3 \times 10^{-19}$ cm^3), we obtain spectra that practically coincide with those in Fig. 3. This is explained by the fact that in Eqn (1) the gain is represented as $G_m(1 - \varepsilon S_m)$; therefore, the photon density in the mode becomes proportional to $G_m \varepsilon S_m^2$, similar to the term γS_m^2.

In the calculations using the system of rate equations [11], it is necessary to use the coefficient $\varepsilon_1 = \varepsilon / \Gamma_a = 2.3 \times 10^{-17}$ cm^3, and γ should be equal to zero. In addition, the calculations assume that $L = 1600$ μm, $\Gamma_a = = 0.0132$, $\Gamma_w = 0.863$, $R_{T0} = 21$ K W^{-1}, $A = 6 \times 10^7$ s^{-1}, $B_{spa} = 8 \times 10^{-11}$ cm^3 s^{-1}, $C_0 = 4.6 \times 10^{-29}$ cm^6 s^{-1}, $\Delta E = 0.46$ eV, $\sigma_e = 3 \times 10^{-18}$ cm^2, $\sigma_h = 35 \times 10^{-18}$ cm^2, $B_{spw} = 8 \times 10^{-11}$ cm^3 s^{-1}, $k_g = 3.8 \times 10^{-8}$ eV cm^{-1}, $D = 8.7 \times 10^{-76}$ cm$^{13.5}$ s^{-1}, $R_1 = 0.05$, $R_2 = 1$.

It should be noted that in work [16], for a strip contact width of 100 μm, the losses $\alpha = 1.3$–1.5 cm^{-1}, while the calculated value of the absorption cross section for holes $\sigma_h = 13.4 \times 10^{-18}$ cm^2 was obtained under the condition that $\alpha = 1.3$ cm^{-1}. In work [10], for a 3 μm wide strip, the losses α constituted 3.3 cm^{-1}, so it was assumed in this work that $\sigma_h = 35 \times 10^{-18}$ cm^2.

Next we consider the effect of the LD thermal resistance on its spectral and power characteristics. In work [19], thermal resistance was calculated by the formula

$$R_T = \frac{1}{k_T}\left(\frac{L_a}{wL} + \frac{L_{sub}}{w_{sub}L}\right), \qquad (22)$$

where $k_T = k_0(T_0/T)^{4/3}$; L_a and L_{sub} are the thicknesses of the active region and the substrate; w_{sub} is the substrate width; and k_0 and k_T are the coefficients of thermal conductivity at temperatures T_0 and T. Thus, tthe hermal resistance R_T increases with increasing LD active region temperature due to a decrease in thermal conductivity. Using formula (22), we obtain $\varkappa = 4/3$. For InP, $\varkappa = 1.5$ [20].

In work [10], a satisfactory agreement between the experimental and calculated light–current characteristic is observed at $\varkappa = 1.4$, i.e. it is assumed that thermal resistance increases with the pump current. The authors of [9] note that thermal resistance decreases with increasing pump current and, by

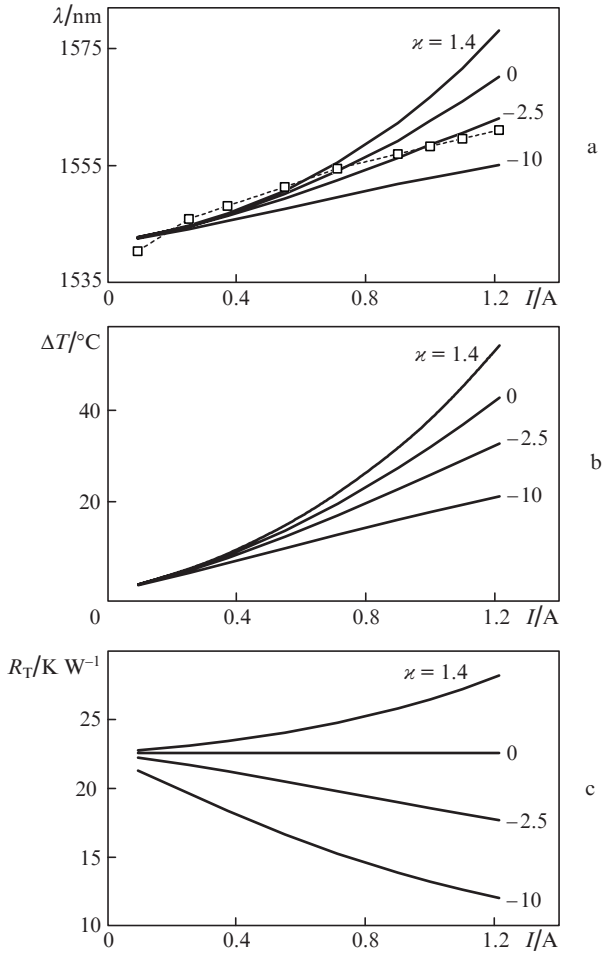

Figure 4. Calculated dependences of (a) the laser wavelength, (b) active region heating, and (c) thermal resistance on the pump current for various values of $\varkappa$. Points in Fig. 4a are the results of the experiment.

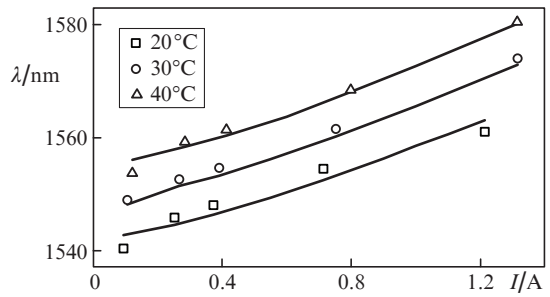

Figure 5. Experimental (points) and calculated (curves) dependences of the laser wavelength on the pump current for various LD radiator temperatures T_0.

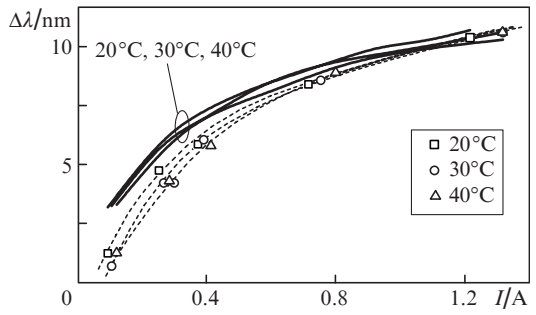

Figure 6. Experimental (points) and calculated (solid curves) dependences of the emission spectrum width on the pump current for various LD radiator temperatures T_0.

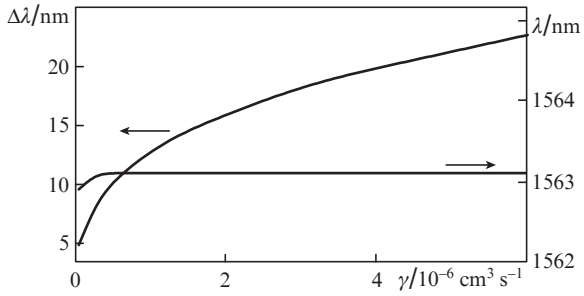

Figure 7. Calculated dependences of the wavelength and emission spectrum width on the coefficient γ at a pump current of 1213 mA (300 mW).

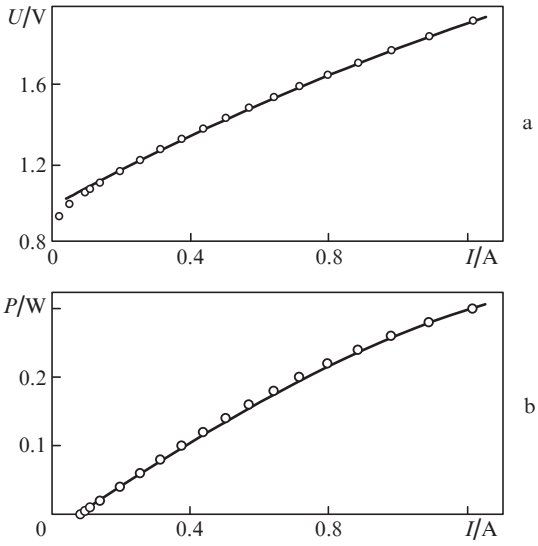

Figure 8. Experimental (points) and calculated (curves) (a) voltage–current and (b) light–current characteristics at $\gamma = 6 \times 10^{-7}$ cm^3 s^{-1}.

definition, depends on the operating point selected for measurement. The dependence of thermal resistance on the pump current is inversely proportional: the higher the current (and, accordingly, the output power), the lower the thermal resistance (even in the ideal case of linear dependence of the wavelength of the spectrum envelope maximum on the pump current). In the present work, the thermal resistance R_T was determined by formula (15), while formula (16) was used to find the active region heating.

As shown by calculations, the laser wavelength at the same radiator temperature strongly depends on the pump current for various values of the coefficient $\varkappa$. The calculated dependences of the laser wavelength on the pump current for $\varkappa = 1.4$, 0, −2.5, and −10 at $T_0 = 20$ °C are shown in Fig. 4a. The larger the $\varkappa$, the greater the radiation wavelength at the same pump current. The best agreement between the calculated data and experiment is observed for $\varkappa = -2.5$. Figure 4b shows the dependence of the LD active region heating on the pump current. It is seen that $\varkappa$ increases with increasing ΔT. The dependences of thermal resistance on the pump current are shown in Fig. 4c. Thermal resistance increases at $\varkappa = 1.4$,

remains unchanged at $\varkappa = 0$, and decreases at $\varkappa = -2.5$ and -10. Analysing the current dependences of the laser wavelength (Fig. 4a) and thermal resistance (Fig. 4b), we can see that at $\varkappa = -10$ (as at $\varkappa = -2.5$), the laser wavelength and the heating of active region increase almost linearly, while thermal resistance decreases with increasing pump current.

For radiator temperatures $T_0 = 20$, 30, and 40 °C, experimental and calculated dependences of the wavelength and emission spectrum width on the pump current coincide with good accuracy (see Figs 5 and 6). From a comparison of these Figures, it follows that the laser wavelength depends stronger on the radiator temperature than the spectrum width.

The calculated dependences of the wavelength and the half-height width of the emission spectrum on the coefficient γ determining the nonlinear losses are given in Fig. 7. It is seen that in contrast to the spectrum width, the laser wavelength is virtually independent of γ. If the γ value is increased by an order of magnitude, the spectrum width increases more than twice. An analysis of the curves in Fig. 7 shows that the dependences of the calculated spectrum width (see Fig. 6) change with increasing or decreasing coefficient γ. The calculated laser wavelength can be varied by changing the coefficient k_g that determines the narrowing of the band gap of the active region E_{ga} when the laser structure is pumped by the current. The emission spectrum width remains unchanged.

Thus, the allowance for nonlinear absorption (or spectral burning of carriers) leads to an expansion of the emission spectra and an increase in the laser wavelength with an increase in the pump current, which agrees with the behaviour of their experimental dependences.

It should be noted that the coefficient γ exerts virtually no effect on the voltage–current and light–current characteristics (see Fig. 8). The calculated value of maximum laser power for $\varepsilon = 0$, $\gamma = 6 \times 10^{-7}$ cm^3 s^{-1} decreases by no more than 2% compared to the case when $\varepsilon = 0, \gamma = 0$.

In work [12], as in the present work, it is noted that a change in the coefficient k_g leads to a shift in the LD wavelength and does not virtually affect the light–current characteristic.

When calculating the voltage–current and light–current characteristics in the framework of the model [10] using characteristic temperatures, the best agreement of the calculated and experimental results is obtained if we assume that the LD thermal resistance increases with the pump current. This model does not allow one to reach a satisfactory agreement between the calculated and experimental voltage–current and light–current characteristics, provided that R_T decreases with increasing I, and to calculate the LD spectral characteristics.

When modelling the voltage–current, light–current, and spectral characteristics with allowance for the radiative and nonradiative recombination of carriers, it is necessary to assume that the LD thermal resistance decreases with increasing pump current. Only in this case we obtain a satisfactory agreement between the calculation and experimental results. The maximum laser power increases with decreasing thermal resistance regardless of whether R_T increases or decreases with increasing I.

Thus, the value of the coefficient $\varkappa$ in formula (15) serves as a fitting parameter that allows us to coordinate the calculated and experimental LD characteristics.

An analysis of the experimental dependence $R_T(I)$ presented in [9] shows that, depending on the pump current, thermal resistance can both increase and decrease.

In work [21], using numerical simulation, heat removal from a high-power LD with a strip contact width of 200 μm and a resonator length of 3 mm is analysed. The contribution to the LD thermal resistance of the main structural elements are considered, and it is shown that the contribution of the copper heat sink constitutes 85%, while the contribution of the housing and base is 15%. Thermal resistance was calculated by the formula

$$R_T = \frac{1}{\pi k_T L} \ln\left(\frac{\pi\sqrt{2}\, D_{HS}}{w}\right) + \frac{t_{HS}}{k_T D_{HS}^2}, \qquad (23)$$

where D_{HS} and t_{HS} are the width and thickness of the heat sink. In contrast to formula (17), formula (23) includes not the LD crystal height h_{LD}, but the heat sink width D_{HS}. The last term in (23) determines the thermal resistance of the heat sink.

In the present work, thermal resistance is determined by two terms: $R_{T0} = R_{LD} + R_{rad}$. Introducing of the value R_{rad} makes it possible to explain a change in the emitter characteristics when various ways of the LD crystal assembling (on the contact plate or on the C-mount) are applied.

4. Conclusions

A satisfactory agreement has been obtained between theory and experiment for the dependences of the wavelength and width of the emission spectrum on the laser pump current with allowance for nonlinear losses or spectral burning of carriers. It has been found that the wavelength, and also the voltage–current and light–current characteristics of the LD are virtually independent of the value γ that determines the nonlinear losses and varies from 0 to 6×10^{-7} cm^3 s^{-1}, whereas the emission spectrum depends strongly on the 6×10^{-7} value.

The effect of LD thermal resistance on the active region heating, wavelength, and LD emission spectrum width is discussed.

References

1. Vinokurov D.A., Zorina S.A., et al. *Fiz. Tekh. Poluprovodn.*, **39**, 388 (2005).
2. Kim J.G., Shterengas L., et al. *Appl. Phys. Lett.*, **81**, 3146 (2002).
3. Lyutetskii A.V., Borshchev K.S., et al. *Fiz. Tekh. Poluprovodn.*, **41**, 883 (2007).
4. Vinokurov D.A., Kapitonov V.A., et al. *Fiz. Tekh. Poluprovodn.*, **41**, 1003 (2007).
5. Tarasov I.S. *Quantum Electron.*, **40**, 661 (2010) [*Kvantovaya Elektron.*, **40**, 661 (2010)].
6. Pikhtin N.A., Tarasov I.S., Ivanov M.A. *Fiz. Tekh. Poluprovodn.*, **28**, 1983 (1994).
7. Slipchenko S.O. et al. *Fiz. Tekh. Poluprovodn.*, **40**, 1017 (2006).
8. Vorob'ev L.E., Zerova V.L., Borshchev K.S., et al. *Fiz. Tekh. Poluprovodn.*, **42**, 753 (2008).
9. Bezotosnyi V.V., Krokhin O.N., Oleschenko V.A., et al. *Quantum Electron.*, **46**, 679 (2016) [*Kvantovaya Elektron.*, **46**, 679 (2016)].
10. Gorlachuk P.V., Ivanov A.V., Kurnosov V.D., et al. *Quantum Electron.*, **48**, 495 (2018) [*Kvantovaya Elektron.*, **48**, 495 (2018)].
11. Bowers J.E., Koch T.L., et al. *Electron. Lett.*, **21**, 393 (1985).
12. Ivanov A.V., Kurnosov V.D., Kurnosov K.V., et al. *Quantum Electron.*, **36**, 918 (2006) [*Kvantovaya Elektron.*, **36**, 918 (2006)].
13. Ivanov A.V., Kurnosov V.D., Kurnosov K.V., et al. *Quantum Electron.*, **37**, 545 (2007) [*Kvantovaya Elektron.*, **37**, 545 (2007)].
14. Adachi S. *Properties of Semiconductor Alloys: Group-IV, III–V and II–VI Semiconductors* (Chichester, UK: John Wiley & Sons, 2009).
15. Grinberg A.A. *IEEE J. Quantum Electron.*, **30**, 1151 (1994).
16. Gorlachuk P.V., Ivanov A.V., Kurnosov V.D., et al. *Quantum Electron.*, **44**, 149 (2014) [*Kvantovaya Elektron.*, **44**, 149 (2014)].
17. Amann M.C. *Appl. Phys. Lett.*, **50**, 4 (1987).
18. Ryvkin B.S., Avrutin E.A. *Appl. Phys.*, **97**, 123103 (2005).
19. Bewtra N. et al. *IEEE J. Sel. Top. Quantum Electron.*, **1**, 331 (1995).
20. Piprek J. *Semiconductor Optoelectronic Devices* (San Diego: Academic Press, 2003).
21. Ter-Martirosyan A.L. et al. *Nauchn. Priborostr.*, **23**, 40 (2013).